ISOLATED MODES AND PERCOLATION IN LATTICE DYNAMICS OF (Be,Zn)Se

A. V. POSTNIKOV,[a*] O. PAGES,[b] T. TITE,[b] M. AJJOUN,[b] and J. HUGEL[b]

[a]*Institute of Metal Physics, S. Kowalewskoj 18, Yekaterinburg 620219, Russia, and Universität Osnabrück – Fachbereich Physik, D-49069 Osnabrück, Germany*
[b]*IPEM, Université de Metz, 1 Bd Arago, F-57078 Metz cedex 3, France*

Abstract

A mixed II-VI semiconductor $Zn_{1-x}Be_xSe$ possesses non-trivial vibration properties, because its two constituent compounds, ZnSe and BeSe, show very different degree of covalency and hence high elastic contrast. An anomalous Be-Se vibration line has been observed mostly at intermediate Be content in the Raman spectra of thin (Zn,Be)Se films. In order to explain microscopic origins and the detailed composition of these lines, a first-principles calculation of vibration frequencies in a mixed crystal has been done, with frozen-phonon technique and supercell setup within the density functional theory, by the SIESTA method, which uses norm-conserving pseudopotentials and strictly localized numerical basis functions. The calculations confirmed an earlier assumption that the anomalous Be-Se line appears due to the formation of continuous chains of a more rigid Be-rich pseudo-continuous phase formed within the more soft Zn-rich host region on crossing the Be-Se bond percolation threshold ($x \sim 0.19$). Different local deformation in percolated and non-percolated regions affect interatomic elastic interactions and split corresponding vibration lines. Besides confirming the percolation model qualitatively, the calculation provides details about vibration patterns in different phonon modes.

*Corresponding author: Tel.: +49 541 969 2377, fax: +49 541 969 2351, email: apostnik@uos.de

1

1. INTRODUCTION

Chalcogenides of Be, characterized by a strong covalent character of their chemical bonding, are outstanding among the II-VI semiconductors which are otherwise largely ionic systems. BeSe makes solid solution with ZnSe in the whole composition region. Beyond providing the possibility to tune the fundamental band gap and dielectric function in broad limits (Wilmers *et al.*, 1999), the coexistence of strongly ionic and strongly covalent bonds in the same crystal makes its elastic and vibrational properties interesting. The frequencies of optical modes in pure ZnSe and BeSe are far separated. This remains basically true in the alloy (Pagès *et al.*, 2000). The remarkable point is that an additional Be-Se mode has been detected, mostly in the intermediate concentration range, 20 to 80 at.% Be. This effect has been tentatively attributed by Pagès *et al.* (2001) to the onset of percolation on the Be sites, i.e., creation of infinite –(Be–Se)– chains in the predominantly ZnSe crystal.

In the attempts to understand and describe the lattice dynamics of mixed crystals in terms of simple models, an obvious difficulty is that interaction parameters (force constants) between two given atoms depend on their local environment in a not straightforward way. The elastic couplings are affected by interatomic distances which may differ in an alloy; moreover the combinatorial aspect (how many neighbours of one or another type) may play an unknown role. Therefore it could be difficult to agree on a simple and yet realistic model. First-principles calculations of lattice vibrations, either by linear response (Pavone *et al.*, 1993; Gonze *et al.*, 1994; Baroni *et al.*, 2001) or frozen-phonon (Wei and Chou, 1992) schemes, work well for perfect crystals (Parlinski and Kawazoe, 1999) or ordered mixed phases (Sternik *et al.*, 1999; Baroni *et al.*, 2001) but face problems in case of substitutional disorder. In this latter case, the treatment of representative supercells remains a virtually unique alternative, with the obvious shortcoming that the selection of such supercells is limited, and the calculation technically demanding. In the present contribution, we calculate electronic structure, force constants and phonon frequencies in the (Zn,Be)Se mixed system using the first-principles method, and calculation code, SIESTA (Soler *et al.*, 2002). The calculations were practically done for Zn_3BeSe_4, $ZnBe_3Se_4$ and $Zn_{26}Be_6Se_{32}$ supercells, the latter simulating both percolating and "isolated" Be ions in the lattice.

The additional vibrational modes, whose appearance in the calculation could be traced back to the onset of percolated Be chains, closely resemble those observed earlier in experimental spectra by Pagès *et al.* (2002b) and outlined briefly in Sec. 2. This supports earlier assumptions about the role of percolation in the formation of split-off vibration lines. The results of calculation, which were organized as described in Sec. 3, allow to study the composition of each vibration mode separately, and to explain the underlying microscopics, in terms of variation of interatomic distances. The discussion of results is given in Sec. 4.

2. EXPERIMENTAL SITUATION

The vibrations spectra of (Zn,Be)Se alloys have been detected by Raman measurements in the backscattering geometry from thin films grown by molecular beam epitaxy on (001) GaAs. The experimental setup, obtained spectra and their discussion have been in detail described earlier (Pagès et al., 2000; Pagès et al., 2001, 2002a). A typical selection of spectra, in dependence on concentrations, is shown in Fig. 1. For the sake of our subsequent discussion,
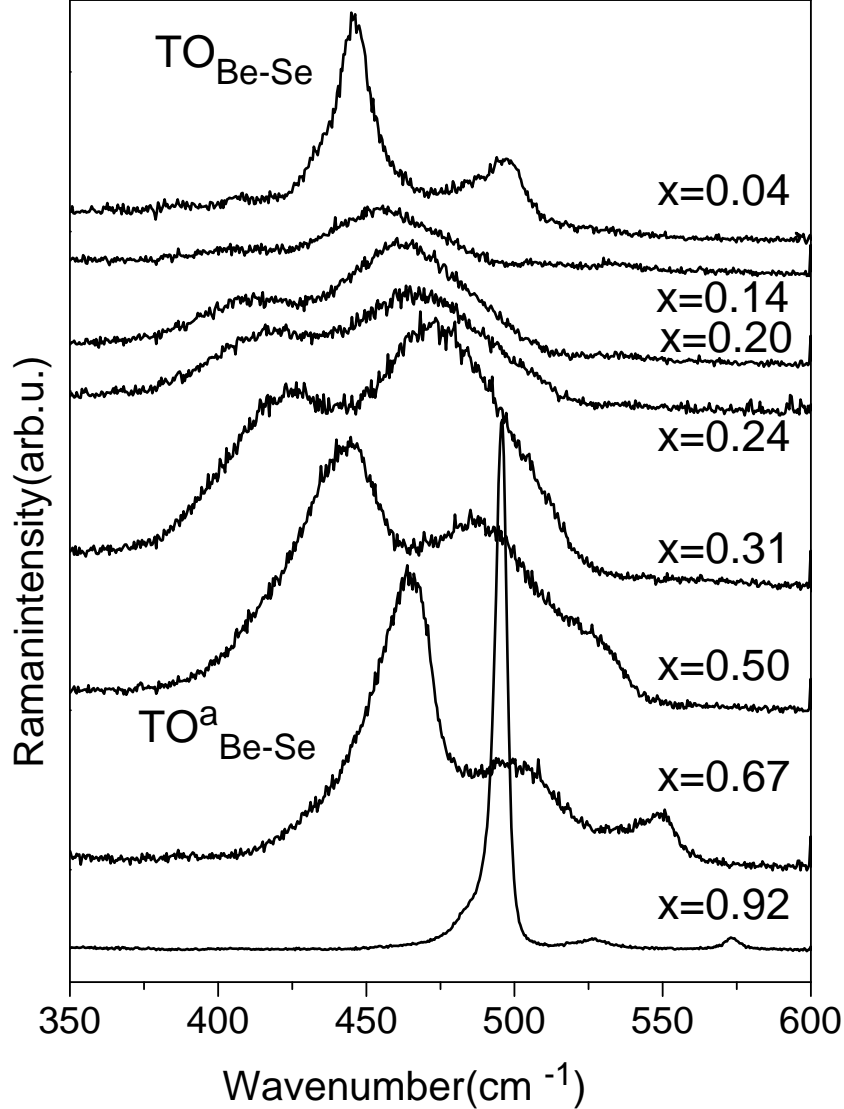

Figure 1: Raman spectra of $Zn_{1-x}Be_xSe$ films grown on the GaAs substrate, measured in the backscattering geometry along the (110) edge axis. The "regular" and "anomalous" (labeled TO^a_{Be-Se}) lines coexist in the concentration range 20 to 80 at.% of Be. See Pagès et al. (2001) for more detailed discussion of the experiment.

we emphasize the region of transverse optical (TO) Be-Se modes, in the range 400–500 cm^{-1}. The Zn–Se mode, around 200 cm^{-1}, is useless because of strong Fano interference with a disorder-activated acoustical continuum (Pagès *et al.*, 2001). Incidentally the large frequency gap between the Be–Se and Zn–Se nodes is basically attributed to the large difference in the reduced mass of two bonds, in the ratio 1:4. The increase in the Be concentration shifts the BeSe-like TO line upwards. From ∼20% of Be on, an additional ("anomalous") peak is formed at ∼70 cm^{-1} on the low-frequency side from the main one. Two peaks coexist through the concentration range ∼20 to ∼80% of Be, both displacing towards higher frequencies and approximately maintaining their separation. The intensity of the anomalous peak grows at the expense of the normal one, until finally (on the Be-rich side) the anomalous peak remains the only one, and ends up as the narrow TO line in the limit of pure BeSe.

The discussion in previous works (Pagès *et al.*, 2001, 2002b) emphasized that such behaviour cannot be accounted for by segregation of crystal into BeSe-rich and ZnSe-rich fractions. The proposed explanation of the anomaly was the following. Above the Be–Se bond percolation threshold (∼19 at.% Be), a pseudo-infinite wall-to-wall chain of Be–Se bonds is formed spontaneously throughout the alloy. Based on simple local strain considerations, the bond length within the chain was presumed to be larger than the bond length of the Be–Se bonds isolated in the ZnSe-like host matrix, with concomitant impact upon the phonon frequencies. However, microscopic justification of this picture was so far lacking. Our present aim is to construct a representative structure model, compare the vibration properties following from it with experimental observations, and in case of agreement to analyze microscopical origins of the observed anomaly.

3. CALCULATION METHOD AND SETUP

First-principles calculations have been performed within the general scope of the density functional theory (see, e.g., Kohn, 1999, for a review), using the calculation method SIESTA (Soler *et al.*, 2002) with its compact basis of strictly confined atom-centered functions (Sánchez-Portal *et al.*, 1996; Junquera *et al.*, 2001). Double-ζ basis functions with polarization orbitals were used for all valence states – Be $2s$ and $2p$, along with $3d$, $4s$ and $4p$ for Zn and Se. Note that we attributed the semicore Se$3d$ states to the valence band. The norm-conserving pseudopotentials have been generated after Troullier and Martins (1991). The results discussed below have been obtained using the local density approximation for the exchange-correlation.

The calculations have been done for three different cubic supercells, shown in Fig. 2. The smaller ones included four formula units in the zincblende structure. BeZn$_3$Se$_4$, with the nominal Be concentration (25 at.%) already beyond the percolation threshold, contained nevertheless only isolated (and
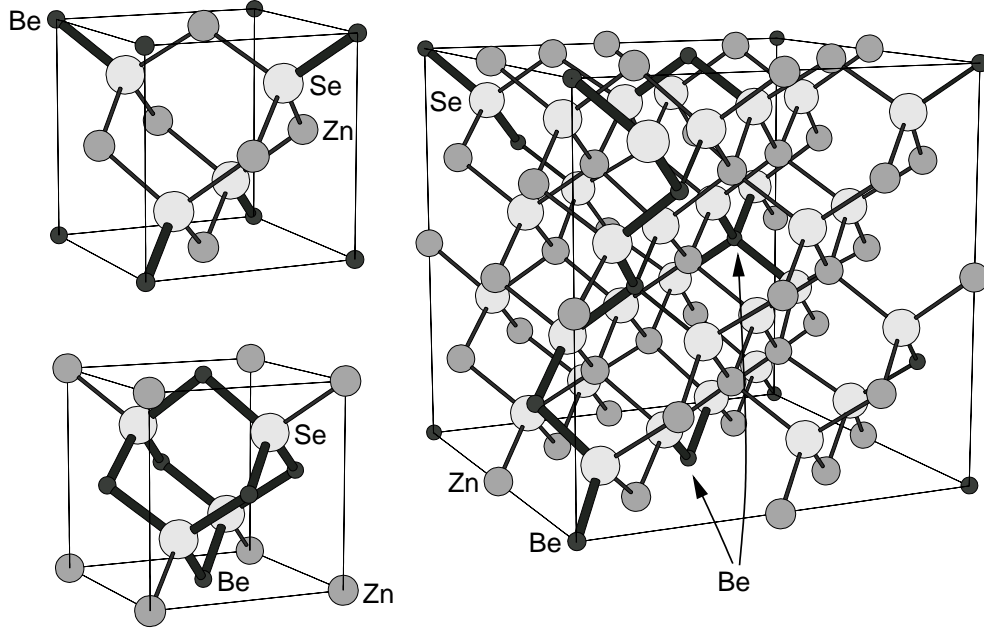
Figure 2: BeZn$_3$Se$_4$, Be$_3$ZnSe$_4$ and Be$_6$Zn$_{26}$Se$_{32}$ supercells used in the calculation. More covalent Be–Se bonds are shown by thick lines. The large supercell contains a continuous (–Be–Se–) chain and two isolated Be atoms (indicated by arrows), who have only Zn atoms as next-nearest neighbours.

artificially ordered) Be impurities, whose second-nearest neighbours are Zn atoms only. The "symmetric" case of 75 at.% Be (Be$_3$ZnSe$_4$) contains, on the contrary, isolated Zn atoms and fully connected Be-Se network. Moreover, a larger supercell Be$_6$Zn$_{26}$Se$_{32}$ simulated the onset of percolation on the Be sublattice, i.e., the formation of continuous (–Be–Se–) chains, along with the presence of isolated Be substitutions. The Be concentration in this case is just above the percolation threshold on the zincblende lattice. In all cases, the calculated forces and strain were used for relaxing the lattice vectors and internal coordinates by the conjugated gradient algorithm, without any symmetry constraints imposed. This allowed us to discuss the variation of the lattice parameters and interatomic distances in their dependence on concentration and local environment. The vibration frequencies have been calculated in the frozen phonon approach, sequentially introducing finite displacements of atoms in the supercell by 0.03 Bohr along three Cartesian directions from their equilibrium positions, and analyzing the forces induced on all atoms. In a single cell, this technique gives access to the zone-center TO phonon only, but in a larger supercell the analysis of phonon eigenvectors allows to make some conclusions about the phonon dispersion.

As benchmarks for testing the quality of the pseudopotentials used and of the basis sets, we calculated the equilibrium lattice parameter and the Γ-TO frequency in pure ZnSe and BeSe. The calculation results are shown

Table 1: Equilibrium lattice constant a, bulk modulus B, and frequency of the Γ-TO phonon ω for pure ZnSe and BeSe from the present calculations (WIEN97 and SIESTA), previous calculations, and experiment.

Method	ZnSe			BeSe		
	a (Å)	B (Kbar)	ω (cm^{-1})	a (Å)	B (Kbar)	ω (cm^{-1})
WIEN97	5.571	727	162	5.087	831	456
SIESTA	5.590	778	200	5.114	965	429
exp.	5.668	624–647	207[a]	5.137[b]	920	501[c]
other calc.		750[d]	216[e]			

[a]Szybowicz *et al.* (2003); [b]Luo *et al.* (1995); [c]Pagès *et al.* (2000); [d]Cohen (1985); [e]Hennion *et al.* (1971)

in Table I along with the experimental data and the results of another, all-electron calculation, which has been performed using an accurate all-electron full-potential linearized augmented plane wave method WIEN97 (Blaha *et al.*, 1997). The difference between the SIESTA results and the experiment reflects the shortcomings of the local density approximation, and moreover technical limitations of the pseudopotential generation and the choice of basis functions. A similarly more faithful estimation of some results with SIESTA, as compared to WIEN97, in view of numerical superiority of the latter method, is probably due to some error cancellation. Anyway, Table I gives an idea of the level of accuracy of our present calculation approach. It is obvious already from comparison the bulk moduli that ZnSe is much softer than BeSe. The same trend holds for the force constants, and mainly accounts for the difference in the Γ-TO phonon frequencies. The difference in Be and Zn masses further enlarges this difference.

4. RESULTS AND DISCUSSION

Fig. 3 shows the calculated equilibrium lattice constant (derived from the volume of relaxed supercells) and nearest-neighbour distances in pure materials and three mixed-composition supercells. One can see that the (Zn,Be)Se lattice parameter quite accurately follows the Vegard's law. At the same time, the Be–Se and Zn–Se bond lengths, which differ by about 9% in the parent compounds, tend to remain diverse, and almost independent on concentration. It means that the accommodation of short Be–Se and long Zn–Se bonds in the lattice of a mixed crystal may lead to local strains and frustrations. In fact, in the large supercell one finds a distribution of bond lengths of one and another
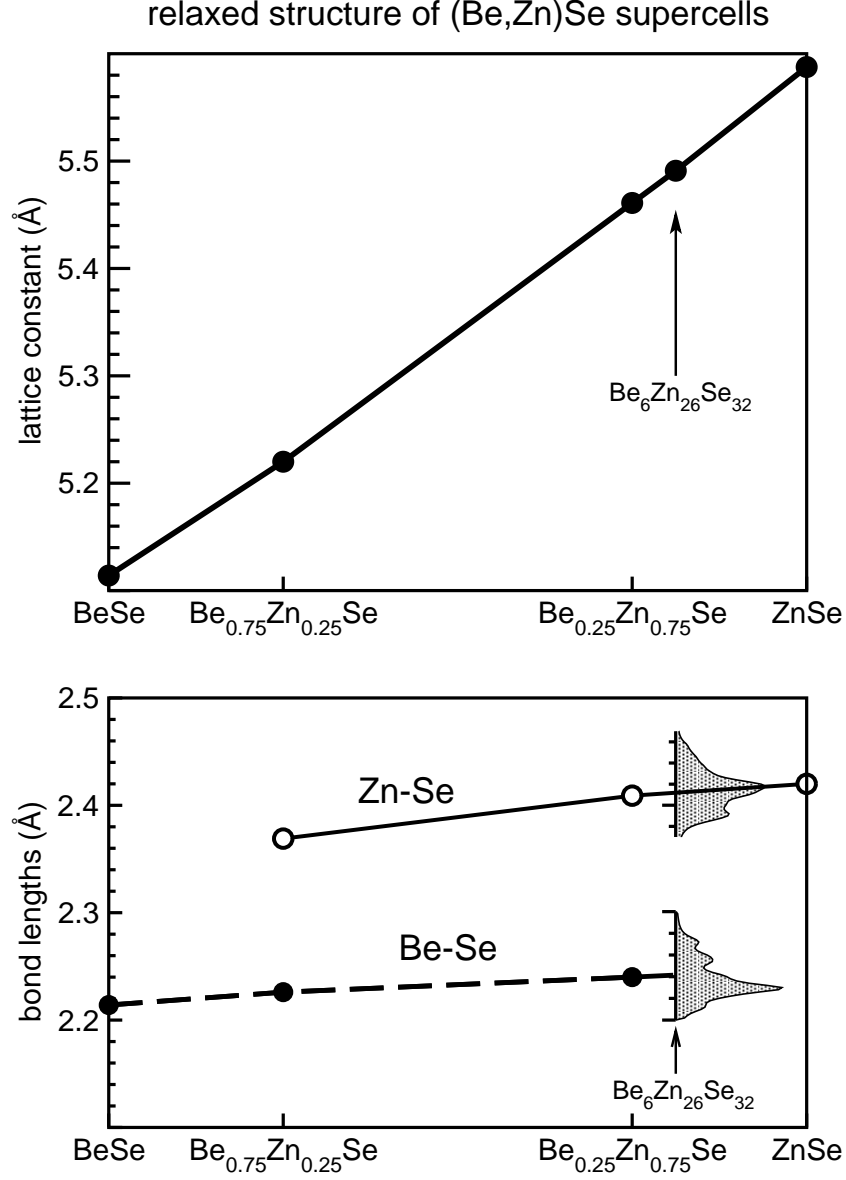
Figure 3: Mean lattice constant (top panel) and nearest-neighbor bond lengths (bottom panel), according to calculations on two pure end systems and three mixed-composition supercells. In the $Be_6Zn_{26}Se_{32}$ supercell, the distribution of Be–Se and Zn–Se bond lengths is shown.

type, shown as continuous curves in the bottom panel of Fig. 3.[1] A further analysis of these different bond lengths shows that isolated (non-chain) Be atoms can easily induce a local and "isotropic" lattice contraction, binding all their four Se neighbours at a distance of 2.23 Å, i.e. at nearly the nominal

---

[1] Obviously the number of nearest-neighbour bonds in the 64-atom supercell is finite (=128); an artificial smearing of the bond distribution function is introduced for better visibility.

bond length of pure BeSe. About the same, or even shorter (2.21 to 2.23 Å), bond length gets stabilized between Be atoms in the chains and their off-chain Se neighbours. One finds finally that the Be–Se bonds *along the chains* are the most difficult to shorten, and exhibit a variation of lengths 2.24 – 2.28 Å. This can be understood because the chain is infinite, and its period is essentially fixed by the mean lattice constant of a crystal with a predominant Zn concentration. The only possibility to shorten the chain links is at the price of increasing the Se–Be–Se angles, making a zigzag chain more straight. This increases average distances between in-chain Se atoms and their Zn neighbours beyond the comfortable ZnSe bond length.

The discussed differences in interatomic distances, and their stretching beyond, or below, the natural bond lengths has an effect on the calculated force constants. A diagonalisation of the dynamical matrix yields frequencies and eigenvectors of all 192 zone-center vibration modes of the supercell, including three acoustic modes (the closeness of whose frequencies to zero is a good test for the numerical accuracy of the calculated forces). Fig. 4 shows phonon densities of states, constructed as

$$n_{\{\alpha\}}(\omega) = \sum_{\{\alpha\}} \sum_i \frac{\Delta}{\pi} \frac{|\mathbf{A}_\alpha(\omega_i)|^2}{\Delta^2 + (\omega - \omega_i)^2} \,,$$

where ω_i are (discrete) vibration frequencies in the supercell (leaving aside the three zero-frequency acoustic modes), $\mathbf{A}_\alpha$ are elements of the eigenvector of the corresponding mode, and the summation is done over $\{\alpha\}$, a selection of atoms in a certain structure category. A broadening parameter $\Delta=10$ cm^{-1} was introduced for better visibility.

The top panel of Fig. 4 shows the contributions of Zn and Be atoms, which are well separated in the frequency domain. The lower part (up to $\sim$300 cm^{-1}) resembles the phonon density of states in ZnSe (see, e.g., Hennion *et al.*, 1971). The high-frequency part represents a Be–Se vibration; its fine structure reveals the differences in the force constants which couple different Be–Se pairs. The vibration modes involving the *isolated* Be are densely situated around 490 cm^{-1}. On the contrary, the vibration bands involving Be atoms in the chains split into a softer and a harder components. A comparison with the phonon DOS projected on Se atoms (Fig. 4, bottom panel) shows that the softer one affects almost exclusively the Se atoms in the chains (i.e those with two Be and two Zn neighbours), whereas the harder one involves also the peripheric Se atoms, which build just one bond to Be in the chains. This separation immediately follows from the distinction between extended Be–Se bonds along the chain, with correspondingly weakened force constants, and "natural" Be–Se bond lengths to off-the-chain Se atoms, or around isolated Be impurities. This observation clearly indicates that the splitting off of a softer "additional" line from the main TO Be–Se peak in the measured spectra (Fig. 1) is due to the formation of continuous (–Be–Se–) chains, where the Be–Se bond length is essentially fixed by the predominantly ZnSe bulk, therefore extended over the
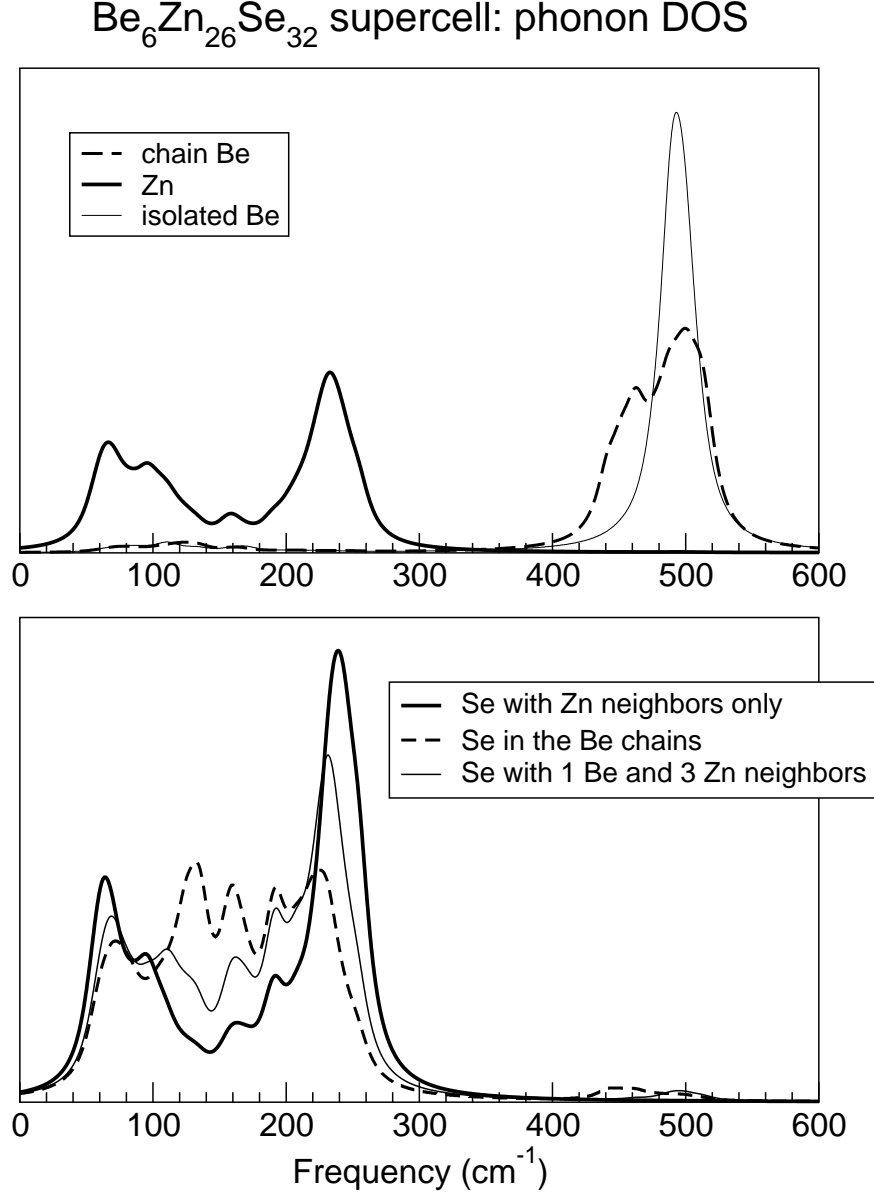
Be$_6$Zn$_{26}$Se$_{32}$ supercell: phonon DOS

Figure 4: Phonon densities of states for different categories of atoms represented in the Be$_6$Zn$_{26}$Se$_{32}$ supercell. Top panel: Be and Zn contributions, bottom panel: Se contributions. Three acoustic modes at $\omega=0$ are removed, and the broadening of discrete vibration lines is introduced.

"natural" Be–Se distance, and results in weakened force constant. The drift of the "normal" and "additional" lines with concentration, seen in Fig. 1, is not directly addressed by our simulation on a single "percolated" supercell, but it can be easily understood from the general trend of the average lattice constant. A gradual shortening of Be–Se distances with the increase in Be concentration hardens *all* vibration modes. The concept of percolation on the Be sublattice also makes clear why the "additional" and not the "normal" mode transforms

into the single TO mode in the limit of high Be concentration (see Fig. 1): the "additional" mode was that involving chained (–Be–Se–) structures, which at high Be concentration become omnipresent.

In order to get a better idea of vibration patterns within "normal" and "additional" lines, we shown in Fig. 5 the snapshots of four vibration modes. Whereas the most of vibration modes involve many atoms in the supercell in a complicated way, these four allow more or less easy understanding of their underlying displacement. Such simplified schemas are shown below each mode, neglecting the bending of the zigzag chain. The most general observation is that the movement of Be atom in the common plane with two Se neighbours occurs at lower frequency than out-of-plane vibrations. This is however a quite simplifying statement; one should consider that the off-the-chain Se atoms also participate in these movements, up to different extent in harder ("normal") and sifter ("additional") modes, as has been mentioned above.

We leave for a subsequent more detailed discussion elsewhere the analysis of vibrations in smaller supercells, which we used here only as a reference to the variation of lattice parameters. Moreover, the analysis of vibration modes with respect to their wave vector is important and will be reported separately, as only $\mathbf{q}=0$ vibrations contribute to the Raman spectra.
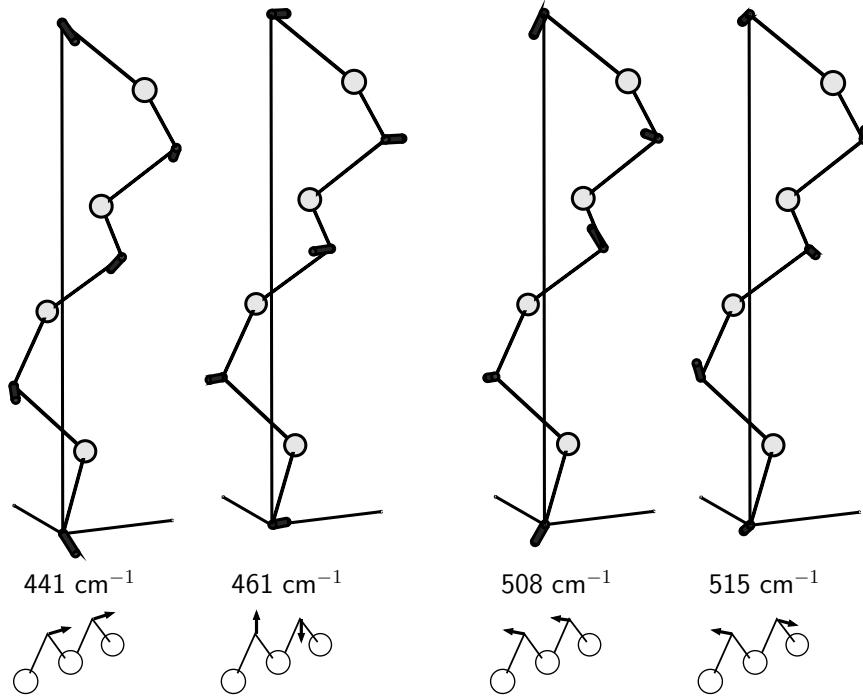

Figure 5: Snapshots of four selected vibration modes involving Be atoms in the chains. The displacements of Se atoms are negligible in the chosen scale. For each mode, a simplified schema of its characteristic displacement is shown below.

5. SUMMARY

By performing a straightforward calculation of vibration frequencies in a large supercell simulating (Zn,Be)Se mixed system, we were able to explain the onset of "anomalous" vibration mode in the frequency range close to the Γ-TO line of BeSe. This mode appears due to a softening of corresponding force constants in expanded Be–Se bonds, that occurs as continuous Be–Se chains start to traverse the $Be_xZn_{1-x}Se$ crystal on reaching the Be percolation limit of $x=19$ at.%. We found remarkable variations of the Be–Se bond length in a (Zn,Be)Se mixed crystal with the Zn predominance. The Be–Se distances shorten most efficiently between Be ions in the percolating chains and their neighbouring Se ions *not* belonging to the chains. On the contrary, the Be–Se distances within the chains are essentially fixed by the ZnSe bulk, i.e. they are over-stretched, as compared to relaxed BeSe crystal. The Be–Se bond length for a Be ion being an isolated substitutional impurity in the ZnSe matrix is intermediate between two previously mentioned cases. As a consequence, one finds distinct Be–Se force constants for these three cases, and hence the splittings of corresponding vibration modes.

References

Baroni, S., S. de Gironcoli, A. Dal Corso and P. Giannozzi (2001). Phonons and related crystal properties from density-functional perturbation theory. *Rev. Mod. Phys.* **73**(2), 515.

Blaha, P., K. Schwarz and J. Luitz (1997). WIEN97, Vienna University of Technology. Improved and updated Unix version of the original copyrighted WIEN-code, which was published by P. Blaha, K. Schwarz, P. Sorantin, and S. B. Trickey, in *Comput. Phys. Commun.* **59**, 339 (1990).

Cohen, M. L. (1985). Calculation of bulk moduli of diamond and zinc-blende solids. *Phys. Rev. B* **32**(12), 7988.

Gonze, X., J.-C. Charlier, D. C. Allan and M. P. Teter (1994). Interatomic force constants from first principles: The case of α-quartz. *Phys. Rev. B* **50**(17), 13035.

Hennion, B., F. Moussa, G. Pepy and K. Kunc (1971). Normal modes of vibrations in ZnSe. *Phys. Lett.* **36A**(5), 376.

Junquera, J., Ó. Paz, D. Sánchez-Portal and E. Artacho (2001). Numerical atomic orbitals for linear scaling. *Phys. Rev. B* **64**(23), 235111.

Kohn, W. (1999). Nobel lecture: Electronic structure of matter – wave functions and density functionals. *Rev. Mod. Phys.* **71**(5), 1253.

Luo, H., K. Ghandehari, R. G. Greene, A. L. Ruoff *et al.* (1995). Phase transformation of BeSe and BeTe to the NiAs structure at high pressure. *Phys. Rev. B* **52**(10), 7058.

Pagès, O., M. Ajjoun, D. Bormann, C. Chauvet *et al.* (2001). Vibrational evidence for a percolative behavior in $Zn_{1-x}Be_xSe$. *Phys. Rev. B* **65**(3), 035213.

Pagès, O., M. Ajjoun, D. Bormann, C. Chauvet *et al.* (2002a). Raman study of $Zn_{1-x}Be_xSe/GaAs$ systems with low Be content ($x \leq 0.20$). *J. Appl. Phys.* **91**(11), 9187.

Pagès, O., M. Ajjoun, J. P. Laurenti, D. Bormann *et al.* (2000). Raman study of $Zn_xBe_{1-x}Se$ alloy (100) epitaxial layers. *Appl. Phys. Lett.* **77**(4), 519.

Pagès, O., M. Ajjoun, J. P. Laurenti, D. Bormann *et al.* (2002b). Vibrational evidence for percolative behavior in ZnBeSe. *Phys. Stat. Sol. (b)* **229**(1), 25.

Parlinski, K. and Y. Kawazoe (1999). *Ab initio* study of phonons in hexagonal GaN. *Phys. Rev. B* **60**(23), 15511.

Pavone, P., K. Karch, O. Schütt, D. Strauch *et al.* (1993). Ab initio lattice dynamics of diamond. *Phys. Rev. B* **48**(5), 3156.

Sánchez-Portal, D., E. Artacho and J. M. Soler (1996). Analysis of atomic orbital basis sets from the projection of plane-wave results. *J. Phys.: Condens. Matter* **8**(26), 3859.

Soler, J. M., E. Artacho, J. D. Gale, A. García *et al.* (2002). The SIESTA method for *ab initio* order-N materials simulation. *J. Phys.: Condens. Matter* **14**(11), 2745. Siesta site: http://www.uam.es/siesta.

Sternik, M., P. T. Jochym and K. Parlinski (1999). Lattice dynamics of $Ga_{1-x}Al_xAs$ studied by ab initio calculations. *Comput. Mater. Sci.* **13**(4), 232.

Szybowicz, M., M. Kozielski, F. Firszt, S. Łęgowski *et al.* (2003). Raman scattering study of ZnBeSe semiconducting mixed crystals. *Cryst. Res. Technol.* **38**(3–5), 359.

Troullier, N. and J. L. Martins (1991). Efficient pseudopotentials for plane-wave calculations. *Phys. Rev. B* **43**(3), 1993.

Wei, S. and M. Y. Chou (1992). Ab initio calculation of force constants and full phonon dispersions. *Phys. Rev. Lett.* **69**(19), 2799.

Wilmers, K., T. Wethkamp, N. Esser, C. Cobet *et al.* (1999). Ellipsometric studies of $Be_xZn_{1-x}Se$ between 3 eV and 25 eV. *Phys. Rev. B* **59**(15), 10071.